Open

Leukemia (2011) 25, 707–737

www.nature.com/leu

LETTERS TO THE EDITOR

A unique three-dimensional SCID-polymeric scaffold (SCID-synth-hu) model for *in vivo* expansion of human primary multiple myeloma cells

Leukemia (2011) **25,** 707–711; doi:10.1038/leu.2010.300;
published online 14 January 2011

Multiple myeloma (MM) cells home to the bone marrow (BM) and adhere to extracellular matrix (ECM) proteins and to bone marrow stromal cells (BMSCs). The close cross talk between MM cells and cells of the non-tumor compartment within the BM has a key role in supporting tumor growth, survival and development of drug resistance. This biological scenario has led to a growing interest in novel drugs, targeting MM cells and/or interfering with their human BM *milieu* (HuBMM).[1,2] Based on this, appropriate *in vivo* models that recapitulate the complex interactions occurring between MM and its HuBMM are required for preclinical evaluation of new anti-MM agents. To date, the *in vivo* study of MM pathobiology and the validation of therapeutic anti-MM agents has been carried out using a variety of models of murine MM or human MM xenografts in immunocompromised mice.[3] These models, however, do not replicate the HuBMM. The development of the SCID (severe combined immunodeficiency)-hu model has been an important advance, as it was the first model to recapitulate a HuBMM in mice.[4–6] However, although the SCID-hu system remains a highly relevant model for preclinical investigation, it does have important limitations: (i) restricted availability of human fetal bone chips; (ii) the allogeneic nature of the fetal BM *milieu* versus MM cells; and (iii) the significant heterogeneity of implanted human bone chips, collected from different individuals at different gestational age, that may produce experimental variability.

With the aim to overcome the limitations of the SCID-hu system, here, we report the development of a novel *in vivo*

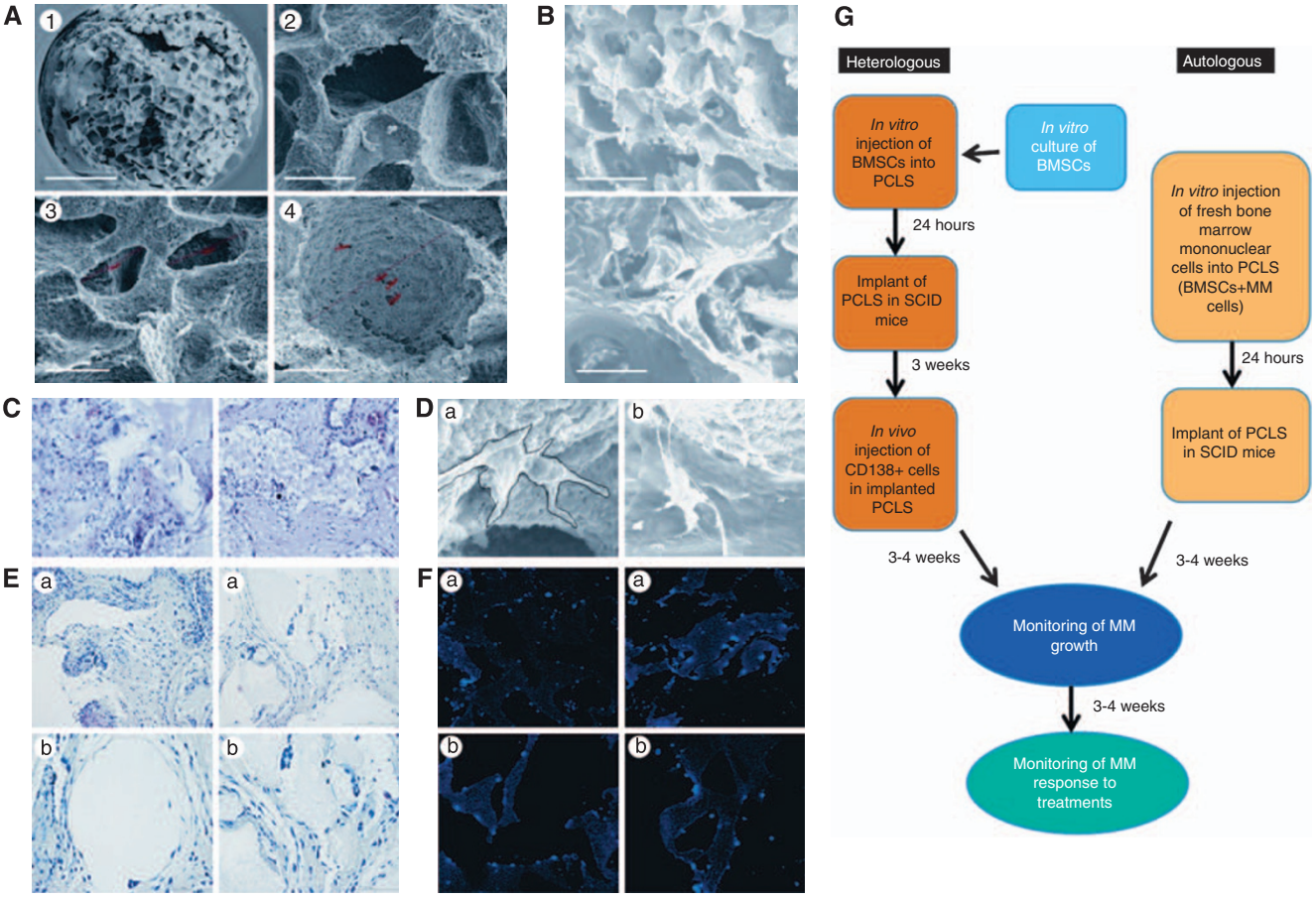

Figure 1 (**A**) SEM analysis of a PCLS (×65 (1), ×500 (2), ×650 (3) and ×1200 (4) magnification) shows interconnected large and small pores (white bars = 1 mm (1), 200 μm (2), 100 μm (3) and 50 μm (4)). (**B**) Comparative SEM analysis (×150 magnification) between a synthetic PCLS (upper panel) and a surgical sample of human femur adult bone (lower panel) shows similar microarchitecture (white bars = 500 μm). Surface morphology was studied by a Leica Cambridge (Stereoscan S440) SEM (Cambridge, UK) at an accelerating potential of 20 kV. (**C**) H&E staining of adherent OP9 mouse stromal cells at 3 weeks after scaffold implant in mice. (**D**–**F**) SEM analysis (×3500 magnification) (**d**), H&E staining (**e**) and confocal laser scanning microscopy (**f**) show adherence within a PCLS of human BMSCs, obtained from two different patients (pt #3, (**a**); pt #7, (**b**) See Table 1), 1 week after implant in mice. (**G**) Flow chart diagram. Schematic representation of experimental methodology.

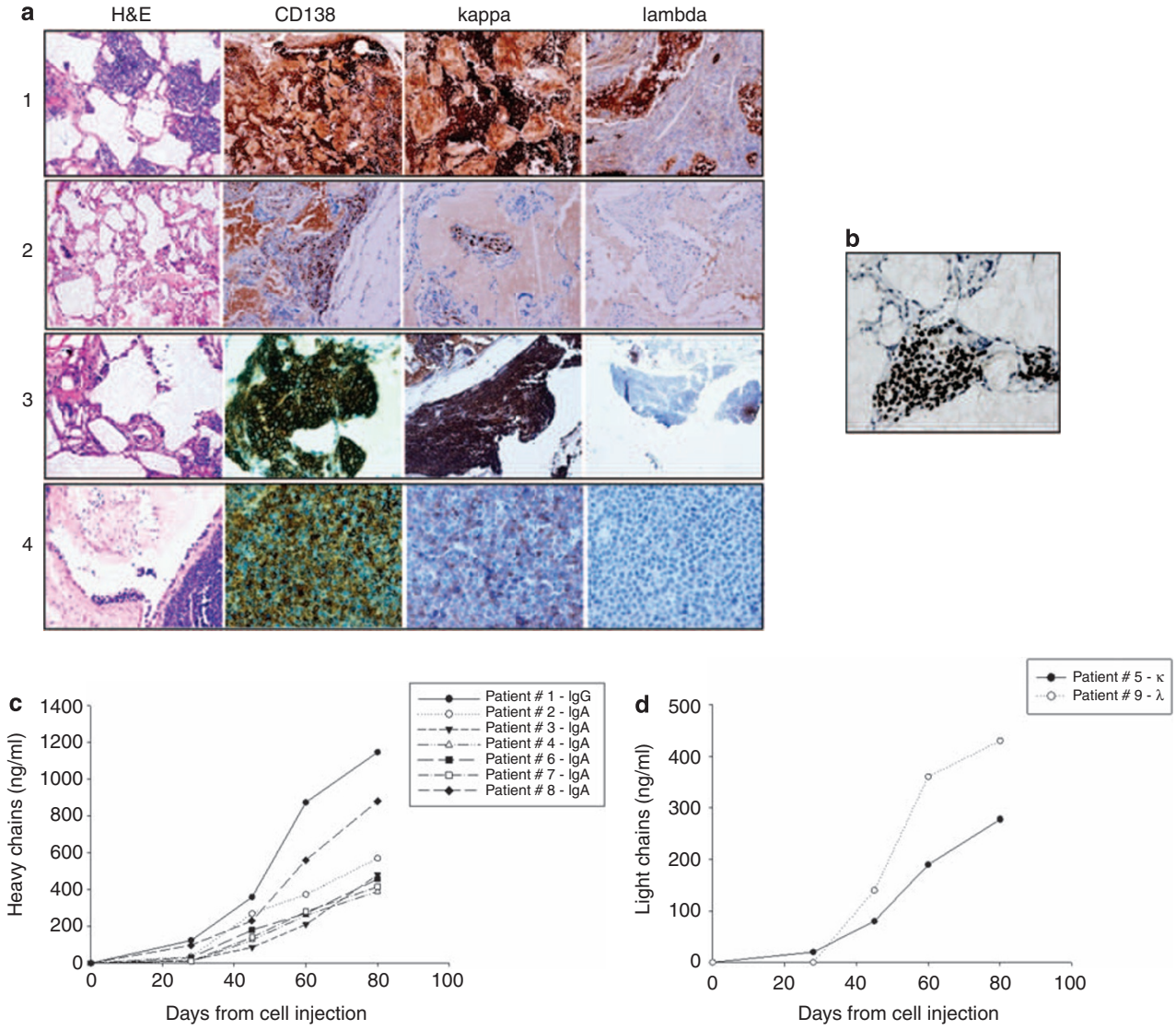

Figure 2 (**a**) Histological and immunohistochemical (anti-CD138/MI15 (Dako, Dako Itala S.p.A., Milano, Italy), anti-κ (Dako) and anti-λ (Dako)) analysis of retrieved PCLSs. Line 1 shows unselected BMMCs; line 2 shows selected CD138+ on heterologous BMSCs; line 3 shows selected CD138+ from PB of a PCL patient on heterologous BMSCs; and line 4 shows IL-6-dependent INA-6 MM cells on heterologous BMSCs. Anti-human κ-light chains and anti-human λ-light chains were used (Dako). Dilutions were 1:15 000 for κ-light chains and 1:10 000 for λ-light chains. (**b**) Ki-67 staining of MM-bearing PCLSs retrieved 3–4 months after cell injection. (**c**, **d**) Kinetics of appearance of paraproteins in sera from representative SCID-synth-hu mice engrafted with samples from MM patients. A code for each patient sample is provided according to Table 1. Left panel includes seven samples from patients with whole paraprotein (ELISA, GenWay Biotech Inc., San Diego, CA, USA); right panel includes two patients with light chain MM (ELISA, Bethyl Laboratories Inc., Montgomery, TX, USA).

human MM model based upon the implantation into a SCID mouse of a three-dimensional (3D) bone-like poly-ε-caprolactone polymeric scaffold (PCLS). In this model, we demonstrated efficient coating of the 3D scaffold internal surface with mouse or human BMSCs and successful engraftment of human primary explanted MM cells within their autologous HuBMM *in vivo*. Using a previously described methodology,[7] we synthesized PCLSs cylinders (7 mm in length and 3 mm in diameter) that, at scanning electron microscope (SEM), demonstrated interconnected large (100–300 μm) and small pores (1–10 μm) (Figure 1A), resembling the microarchitecture of a normal human femur adult bone (Figure 1B). PCLSs were stored at 4 °C in ethanol 70% and then were maintained overnight in 50 ml of sterile water before use. In these PCLSs, we first seeded OP9 cells, a mouse BMSC line, to set up the experimental loading conditions. As OP9 cells efficiently adhered to 3D surfaces (Figure 1C), we next evaluated the suitability of these PCLSs to host human BMSCs derived from MM patients. OP9 mouse BMSCs were cultured in α-MEM (GIBCO, Invitrogen, San Giuliano Milanese (MI), Italy) containing 10% heat-inactivated fetal bovine serum. Human BMSCs were obtained with long-term culture (28 days) of bone marrow mononuclear cells (BMMCs) from Ficoll gradient separation of BM aspirates.[8] Dynamic seeding of BMSCs into PCLSs was performed *in vitro* using a suspension of 10^6 cells in 500 μl of growth medium. A 22-gauge needle on a 2.5 ml syringe was threaded into two ending face of the cylindrical scaffold. A medium flow rate of 500 μl/min and three drawing cycles were carried out on both scaffold ends. Before implantation, PCLSs were incubated in complete medium at 37 °C in 5% CO_2

for 24 h to allow cell adhesion on 3D surfaces. Then, the PCLS was surgically implanted subcutaneously into a SCID mouse flank. Chloralium hydrate anesthesia (400 mg/kg) was used during all surgical procedures. Figure 1G shows the flow chart diagram of experimental procedures. As shown in Figures 1D–F, cultured human BMSCs adhered and spreaded among 3D interconnected surfaces, starting 1 week after cell injection, as demonstrated by SEM, hematoxylin and eosin (H&E) staining and confocal laser scanning microscopy. Based on these achievements, we next evaluated the suitability of these BMSCs-coated PCLSs for engraftment of primary MM cells and interleukin-6 (IL-6)/BM-dependent INA-6 MM cell line. $CD138^+$ immunoselected primary MM cells from BM aspirates of patients with newly diagnosed ($n=5$) or plasma cell leukemia (PCL, $n=1$), and from peripheral blood of PCL patients ($n=2$), as well as INA-6 cells were injected *in vivo* in previously implanted PCLSs that, 3 weeks before, were coated *ex vivo* with BMSCs. Importantly, although both primary MM cells and IL-6/BM-dependent INA-6 MM cells successfully engrafted in human BMSCs-coated PCLSs, they did not engraft into scaffolds previously coated with murine BM stromal cell line OP9 or empty PCLSs. This finding is in agreement with previous observations in the SCID-hu model, where primary MM or INA-6 cells did not infiltrate mouse bone or other murine organs.[5,6] These observations suggest that species-specific interactions allow MM *in vivo* growth in our system.

With the aim to overcome one of the important limitations associated with the SCID-hu model, we further attempted to engraft primary MM cells within their autologous HuBMM. To achieve this aim, we injected unselected BMMCs, obtained by Ficoll gradient separation of BM aspirate of MM patients, into PCLSs. This unselected BMMC suspension, containing both primary $CD138^+$ MM cells and their autologous BMSCs, was freshly seeded *ex vivo* in uncoated PCLSs before *in vivo* implantation of the scaffold in SCID mouse flank (Figure 1g, flow chart diagram). Notably, we achieved a successful engraftment of all patient samples (Figure 2, Table 1). Clinical features of donor MM patients and the actual rate of MM engraftment in SCID-synth-hu mice are reported in Table 1. As shown in Figure 2a, retrieved PCLSs from SCID-synth-hu mice injected with $CD138^+$ immunoselected primary MM cells or unselected BMMCs containing primary MM cells, or INA-6 MM cells demonstrated engraftment and filling of 3D spaces by tumor cells, as confirmed by both H&E and CD138 or κ/λ staining. As we observed slow progressive degradation of PCLSs in mice, long-term survival of MM cells and active proliferation were demonstrated by Ki-67 staining 3–4 months after cell injection (Figure 2b). Following 3–4 weeks, MM cell growth was monitored *in vivo* by enzyme-linked immunosorbent assay detection of human heavy or light chains in mouse sera (Figures 2c and d). Moreover, to assess the suitability of this model for preclinical evaluation of anti-MM agents, we next treated MM-bearing SCID-synth-hu mice intraperitoneally with bortezomib (on days 1, 4, 8 and 11) and dexamethasone (on days 1–4). Such regimen dramatically inhibited MM cell growth *in vivo*, as demonstrated by the fall of paraprotein levels in mouse sera (Figure 3a) and by the detection of MM cell apoptosis in retrieved PCLSs (Figure 3b), as compared with untreated control mice. These results clearly demonstrated that this model is actually suitable for large-scale *in vivo* preclinical screening of investigational anti-MM drugs. An additional important observation was the detection of vasculogenetic events in retrieved PCLSs. In fact, H&E and immunohistochemical staining demonstrated vasculogeneic activity together with the presence of a neosynthesized ECM (Figure 3c). Both in

Table 1 Clinical features of MM patients and PCLS engraftment

Patient code	*Gender*	*Disease status*	*Samples origin*	*Percentage of BM infiltration*	*Previous therapy*	*Isotype*	*Cells injected*	*Number of mice engrafted/injected*
# 1	M	MM in leukemic phase	PB		VAD+ASCT/Vel–Dex/EPT	IgG κ	2×10^6 (selected 138+ cells)	6/7 selected (138+ cells)
# 2	M	Untreated	BM	53	None	IgA λ	1.2×10^6 (selected 138+ cells)/ 3×10^6 (unselected)	3/3 selected (138+ cells) and 2/2 unselected
# 3	M	Untreated	BM	35	None	IgA κ	0.6×10^6 (selected 138+ cells)/ 4×10^6 (unselected)	4/5 selected (138+ cells) and 2/2 unselected
# 4	M	Relapsed	BM	22	VAD/MP/Vel–Dex	IgA λ	4×10^6 (unselected)	5/5 unselected
# 5	M	Untreated	BM	48.50	None	κ-Light chain	2×10^6 (selected 138+ cells)	6/8 selected (138+ cells)
# 6	M	Untreated	BM	30	None	IgA κ	0.7×10^6 (selected 138+ cells)	6/7 selected (138+ cells)
# 7	F	Untreated	BM	30	None	IgA κ	0.7×10^6 (selected 138+ cells)	5/5 selected (138+ cells)
# 8	F	Untreated	BM	15	None	IgG λ	1.5×10^6 (unselected)	9/11 unselected
# 9	F	MM in leukemic phase	BM and PB	80	MP/Vel–Caelyx/LP	λ-Light chain	1.5×10^6 (selected 138+ cells)/ 1.5×10^6 (unselected)	4/4 selected (138+ cells) and 4/5 unselected

Abbreviations: ASCT, autologous stem cell transplantation; BM, bone marrow; EPT, endoxan prednisone and thalidomide; LP, lenalidomide and prednisone; MP, melphalan and prednisone; PB, peripheral blood; VAD, vincristine doxorubicin and dexamethasone; Vel–Dex, bortezomib and dexamethasone.

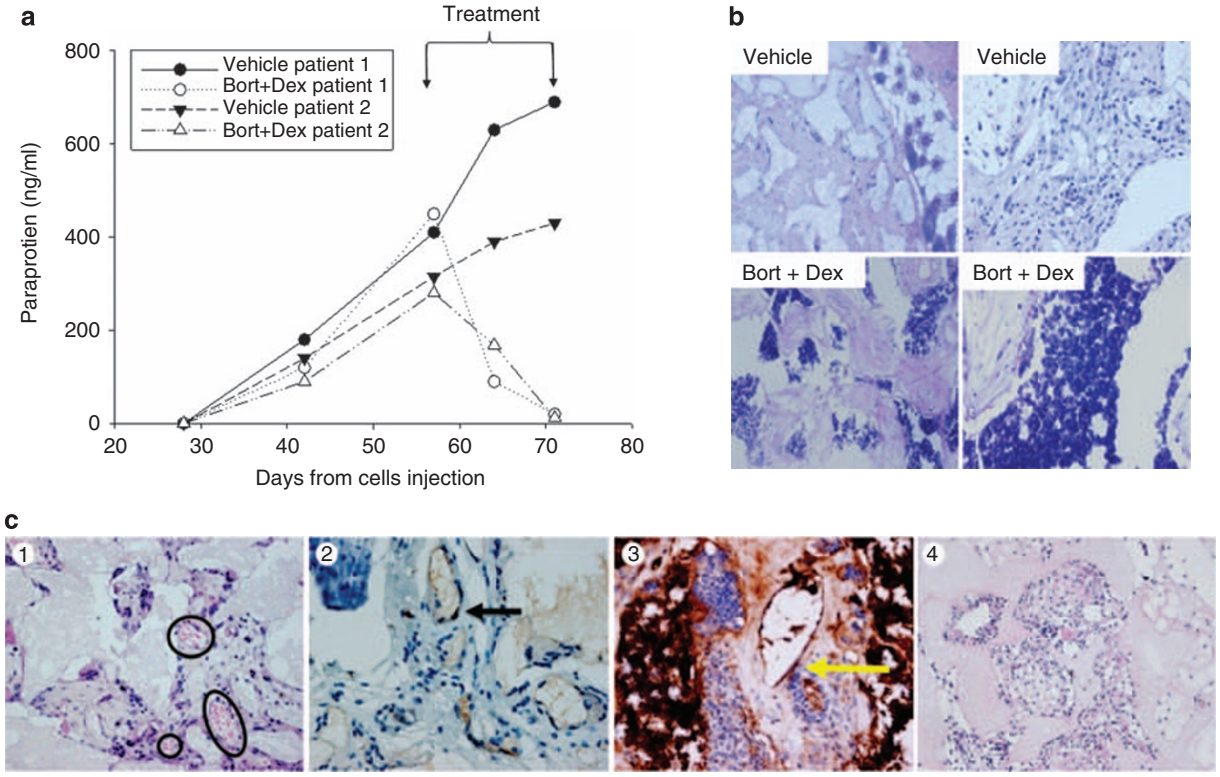

Figure 3 (**a**) SCID-synth-hu mice were treated intraperitoneally with bortezomib (1 mg/kg) + dexamethasone (1 mg/kg). The black arrows indicate the time of treatment. (**b**) H&E staining of a MM-bearing PCLS, engrafted with primary MM cells, following Bort + Dex treatment showed diffuse stromal and intracellular calcification demonstrating massive apoptosis. (**c**) (**1**) H&E staining of a retrieved PCLS showed vessels of variable size (black circles). (**2**) Immunohistochemistry of a PCLS coated with BMSCs demonstrated reactivity with an anti-CD31/JC70A (Dako) specific for human CD31 (black arrow). Appropriate positive control tissues were added on each automated immunohistochemistry run to confirm antibody specificity. Negative control section included normal rabbit serum as a substitute for the primary antibody. (**3**) H&E staining of a retrieved PCLS engrafted with BMMCs shows an active site of vasculogenesis within an area of MM cell growth (yellow arrow). (**4**) H&E staining of a retrieved PCLS coated with BMSCs revealed the presence of a neosynthesized ECM inside the pores.

BMSCs-coated PCLSs injected with MM cells and in scaffolds directly implanted with BMMCs, we observed vessels of variable size and human-derived endothelial cells as demonstrated by reactivity of a specific anti-human CD31 mAb. The vasculogenetic activity mostly occurred within areas of MM infiltration (Figure 3 c3). These findings suggest a role of human vasculogenesis in our system.

All together, our findings demonstrate that the SCID-synth-hu is a novel model for *in vivo* engraftment of human primary MM cells within their autologous adult HuBMM. This model offers several potential advantages as compared with the SCID-hu system that includes the unlimited availability of PCLSs, the ability to dissect biological events within the HuBMM and, most importantly, the engraftment of primary MM cells in a non-fetal adult autologous HuBMM. Moreover, the present model represents the first system for *in vivo* expansion of human MM cells on a synthetic platform. We conclude that the SCID-synth-hu is a unique tool for large-scale *in vivo* preclinical evaluation of novel agents targeting MM in an autologous HuBMM and a novel resource for translational research in the experimental treatment of this still incurable disease.

Conflict of interest

The authors declare no conflict of interest.

Acknowledgements

This work was supported by the Italian Association for Cancer Research (P.T. project, 2007–2009, P.N. project, 2008–2010, and P.T. Special Program Molecular Clinical Oncology -5 per mille, 2010–2015), Milan and the Italian Ministry of Education, PRIN (P.T. project, 2007–2008), Italy.

T Calimeri[1], E Battista[2,3], F Conforti[4], P Neri[1,5], MT Di Martino[1], M Rossi[1], U Foresta[1], E Piro[6], F Ferrara[7], A Amorosi[4], N Bahlis[5], KC Anderson[8], N Munshi[8], P Tagliaferri[1], F Causa[2,3] and P Tassone[1]

[1]*Translational Medical Oncology Unit, Department of Experimental and Clinical Medicine, University of Magna Græcia and Tommaso Campanella Cancer Center, Catanzaro, Italy;*
[2]*Biomaterials Laboratory, Department of Experimental and Clinical Medicine, University of Magna Græcia, Catanzaro, Italy;*
[3]*Center for Advanced Biomaterials for Health Care, Italian Institute of Technology, Napoli, Italy;*
[4]*Department of Pathology, School of Medicine, University of Magna Græcia, Catanzaro, Italy;*
[5]*Department of Medicine, Hematology Unit, University of Calgary, Calgary, AB, Canada;*
[6]*Hematology Unit, Azienda Ospedaliera Pugliese-Ciaccio, Catanzaro, Italy;*
[7]*Orthopedic Surgery Unit, Villa Serena Hospital, Catanzaro, Italy and*

[8]Jerome Lipper Multiple Myeloma Center, Dana-Farber Cancer Institute & Harvard Medical School, Boston, MA, USA
E-mail: tassone@unicz.it

References

1 Kyle RA, Rajkumar SV. Multiple myeloma. *N Engl J Med* 2004; **351**: 1860–1873.
2 Tassone P, Tagliaferri P, Fulciniti MT, Di Martino MT, Venuta S. Novel therapeutic approaches based on the targeting of microenvironment-derived survival pathways in human cancer: experimental models and translational issues. *Curr Pharm Des* 2007; **13**: 487–496.
3 Dalton W, Anderson KC. Synopsis of a roundtable on validating novel therapeutics for multiple myeloma. *Clin Cancer Res* 2006; **12**: 6603–6610.
4 Urashima M, Chen BP, Chen S, Pinkus GS, Bronson RT, Dedera DA *et al.* The development of a model for the homing of multiple myeloma cells to human bone marrow. *Blood* 1997; **90**: 754–765.
5 Yaccoby S, Barlogie B, Epstein J. Primary myeloma cells growing in SCID-hu mice: a model for studying the biology and treatment of myeloma and its manifestations. *Blood* 1998; **92**: 2908–2913.
6 Tassone P, Neri P, Carrasco DR, Burger R, Goldmacher VS, Fram R *et al.* A clinically relevant SCID-hu *in vivo* model of human multiple myeloma. *Blood* 2005; **106**: 713–716.
7 Causa F, Netti PA, Ambrosio L, Ciapetti G, Baldini N, Pagani S *et al.* Poly-epsilon-caprolactone/hydroxyapatite composites for bone regeneration: *in vitro* characterization and human osteoblast response. *J Biomed Mater Res A* 2006; **76**: 151–162.
8 Fulciniti M, Tassone P, Hideshima T, Vallet S, Nanjappa P, Ettenberg SA *et al.* Anti-DKK1 mAb (BHQ880) as a potential therapeutic agent for multiple myeloma. *Blood* 2009; **114**: 371–379.

Differential expression of the *BCR* gene in sequential stages of murine hematopoietic hierarchy

Leukemia (2011) **25,** 711–713; doi:10.1038/leu.2010.303; published online 14 January 2011

The recent manuscript by Marega *et al.*[1] entitled 'BCR and BCR-ABL regulation during myeloid differentiation in healthy donors and chronic phase/blast crisis chronic myeloid leukemia patients', which reported the BCR expression during the different stages of maturation of human myeloid cells provides important insight into the nature of chronic myeloid leukemia, particularly the similarity of BCR and BCR-ABL differential expression patterns during myeloid maturation in healthy subjects and patients with chronic-phase chronic myeloid leukemia, respectively. We studied the expression of BCR transcripts in the murine hematopoiesis. Similar to Marega *et al.*, we found that BCR is differentially expressed during murine hematopoietic maturation. Further, our findings begin to address one of the conundrums ensuing from the work by Dr Eaves and her team in which it was reported that BCR-ABL transduction of mouse bone marrow resulted in expansion of granulocytes, lymphocytes and erythrocyte.[2]

In fact, we performed our quantitative BCR transcript expression analysis in detailed stages of the murine hematopoietic hierarchy by assessing RNA obtained from single-cell progenitors with known fate, a strategy that has been previously published.[3–6] The different stages of murine hematopoiesis that were analyzed included the long-term repopulating hematopoietic stem cells (LTR-HSCs) that are characterized by the phenotype (Rho^{lo}/Kit^+/$Sca1^+$/Lin^-/$CD49b^{lo}$) and able to repopulate the entire hematopoietic system for more than a year,[6] the intermediate-term repopulating hematopoietic stem cells (ITR-HSCs) that have the phenotype (Rho^{lo}/Kit^+/$Sca1^+$/Lin^-/$CD49b^{hi}$) and are able to repopulate the entire hematopoietic system for 3–12 months,[6] the multipotent B+ (which have clonal potential erythroid (E), megakaryocytic (Meg), macrophagic (Mac), neutrophilic (Neut), mastocytic (Mast) and B lymphocyte (B)), pentapotent (with the potential E, Meg, Mac, Neut and mastocytic), the tetrapotent (with the potential E, Meg, Mac and Neut), the bipotent (pE/pMeg and pNeut/pMac), the unipotent (burst-forming unit-erythroid, colony-forming unit-erythroid, pMeg, pMac and pNeut) progenitors and, finally, the terminally differentiated cells (E, Meg, Mac, Neut, mastocytic, B and T); the lineage potentials of the different cells sampled are summarized in Figure 1a. Complementary DNA was obtained from sorted cells (LTR-HSCs, ITR-HSCs, mature B and mature T) or pooled from single cells, differentiation potential of which was determined by the outcome of cultured sibling cells (the multipotent B+, the pentapotent, the tetrapotent, the bipotent, the unipotent and the terminally differentiated cells). In addition, we also analyzed *BCR* gene transcript levels in HSCs that were harvested from normal marrow in G0 phase and after stimulation, with Kit ligand, Flt3 ligand and IL-11, in culture to undergo mitosis. Furthermore, we compared BCR expression in LTR-HSCs and ITR-HSCs at entry into cell cycle (G1 phase) and again at a point when half of the cells had undergone mitosis (M phase); the distinction between these two stages was done on the basis of morphological criteria.

Indeed, high BCR transcript levels were seen in LTR-HSCs and interestingly in the pE/Meg progenitors (BCR/glyceraldehyde-3-phosphate dehydrogenase of 0.008 and 0.0093, respectively) (Figure 1a and b), intermediate levels were found in ITR-HSCs and pentapotent and pNeut/Mac cells (BCR/glyceraldehyde-3-phosphate dehydrogenase ratios of 0.0022, 0.001 and 0.002, respectively), whereas low levels were detected in pMeg, pMac, pNeut, Meg and Neut (0.000231, 0.000073, 0.000239, 0.000158 and 0.000169) (Figure 1a and b). Finally, BCR Expression was not detected in the multipotent B+, tetrapotent, burst-forming unit-erythroid, colony-forming unit-erythroid and the terminally-differentiated cells (E, Mac, mastocytic, B and T) (Figure 1a and b). We also analyzed *BCR* gene transcript levels in HSCs that were harvested from normal marrow in G0 phase and after stimulation, in culture to undergo mitosis. Interestingly, when BCR transcript levels were compared in LTR-HSCs and ITR-HSCs harvested from normal marrow in G0 phase and after stimulation to undergo mitosis, cycling LTR-HSCs and ITR-HSCs showed 7.6- and 4.3-fold increase, respectively, in BCR transcripts (Figure 1c).

Although we used different methodology for defining the different stages of hematopoietic maturation, our results indicate that the expression of BCR during the different stages of murine hematopoiesis are consistent with the results reported by Marega *et al.*